Integrated Electroplated Micromachined Magnetic Devices Using Low Temperature Fabrication Processes

Jae Yeong Park, *Member, IEEE,* and Mark G. Allen

***Abstract*—Micromachining techniques are used to realize inductors and transformers integrated with a multichip package, allowing compact integration with chips, sensors, and other components. The processing steps chosen are all low-temperature, which allows the use of low cost substrates such as MCM-L compatible materials. A variety of micromachined inductors and transformers with different geometries and magnetic core materials are designed, fabricated, tested, and compared. Integrated permalloy and orthonol core inductors (15 μm thick) with nominally identical geometries of 4 mm × 1.0 mm × 0.13 mm and 30 turns of multilevel copper coils (40 μm thick) show differences in performance due to differences in core behavior. The permalloy core inductor has a slightly higher inductance, but it has much lower dc saturation current than the orthonol core inductor. The effect of insertion of a core air gap was also studied. Although inductors with no air gap having dimensions of 4 mm × 4 mm × 0.145 mm and 156 turns of multilevel electroplated copper coils (40 μm thick) and electroplated permalloy magnetic core (35 μm thick) have slightly higher inductance (about 1.5 μH), air gap inductors have much higher saturation current (I80 = 250 mA). These devices have high current capability (up to 3 A steady dc current) and are suitable for low power converter applications.**

***Index Terms*—DC saturation current, electroplating, integration, low temperature process, micromachined inductors, micromachined transformers, orthonol, permalloy, power magnetic devices.**

I. Introduction

MICROMACHINED magnetic devices which have low resistance and high values of inductance, Q-factor, coupling factor, and saturation current are useful in many applications such as miniaturized sensors, actuators, filters, and switched power converters integrated with multichip modules or electronic systems [1]–[5]. In particular, the use of these devices is necessary to miniaturize dc/dc converters used as power supplies in communications, military/aerospace applications, and computer/peripheral or other portable devices. Miniaturized dc/dc converters using micromachined inductors and transformers have many potential advantages such as high frequency operation, efficiency, quality, low cost, and low power loss [6]–[8]. At high switching frequencies, miniaturized surface-mount magnetic components may be able to be replaced by fully integrated magnetic devices [9], [10].

Manuscript received January 30, 1998; revised October 19, 1999. This work was supported by the National Science Foundation through the Georgia Tech/NSF Engineering Research Center in Electronic Packaging under Contract EEC-9402723, E. I. DuPont de Nemours & Co., and M&T Chemicals, Inc.

J. Y. Park is with the Microsystem Team, Devices and Materials Laboratory, LG Corporate Institute of Technology, Seoul 137-724, Korea (e-mail: jpark41@lgcit.com).

M. G. Allen is with the School of Electrical and Computer Engineering, Georgia Institute of Technology, Atlanta, GA 30332 USA (e-mail: mallen@ece.gatech.edu).

Publisher Item Identifier S 1521-334X(00)01469-5.

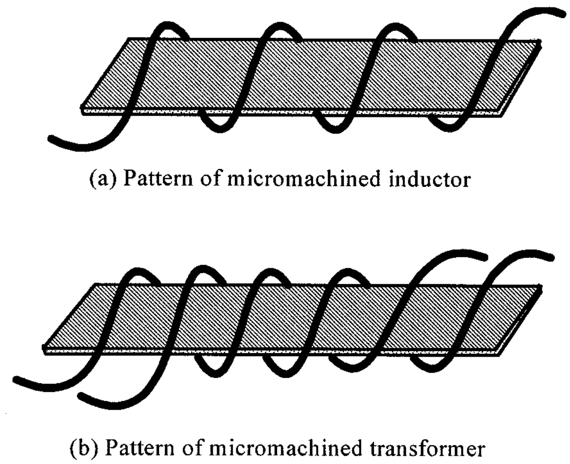

Fig. 1. Conceptual drawing of micromachined inductors and transformers.

Desirable characteristics of magnetic cores for integrated power inductors and transformers can be summarized as follows: first, high saturation flux in order to obtain high saturation current; second, high permeability to obtain high inductance; third, high resistivity to reduce eddy current loss at high frequency. In addition, micromachined magnetic devices should be designed to have a completely closed magnetic circuit to minimize leakage flux, since leakage flux does not contribute to the total inductance of the devices and can cause interference with other integrated circuitry on the same substrate. Magnetic properties of electroplated cores for such devices may be very different from magnetic properties of the bulk magnetic materials, thus necessitating an *in situ* property assessment. Our approach is to fabricate these required inductive components using low-temperature micromachining techniques in order to enable low-cost, fully integrated versions of these power converter devices [11].

II. Design Issues

Fig. 1 shows a conceptual view of micromachined magnetic devices which are composed of a magnetic core and multilevel metal conductors. The micromachined magnetic devices are designed to have a completely closed magnetic circuit to minimize leakage flux and an airgap is optionally included in the magnetic core to desensitize the device properties to applied field and to increase the saturation current [12]–[15]. Electroplating techniques are used to fabricate the conductor lines and the vias, as electroplated metal contacts usually have a relatively low metal contact resistance. The reluctance ($\Re$) and inductance (L) are calculated by the following equations:

$$\Re = \frac{\ell_c}{\mu_0 \mu_r A_c} \tag{1}$$

$$L = \frac{\mu_0 \mu_r A_c N^2}{\ell_c} = \frac{N^2}{\Re} \tag{2}$$

where

- A_c cross-sectional area of the film magnetic core;
- ℓ_c length of the closed magnetic core;
- N number of coil turns;
- $\mu_0\ \mu_r$ permeability of vacuum and then relative permeability of the magnetic core.

The quality factor and dc resistance can be defined as

$$Q = \frac{\omega L}{R}, \qquad R = \rho \frac{\ell_w}{A_w} \tag{3}$$

where

- A_w cross-sectional area of the conductor;
- ω radian frequency;
- ℓ_w length of the conductor lines;
- ρ resistivity of the conductor material.

From the above (2) and (3), it is seen that inductance and Q-factor are linearly proportional to μ_r and A_c in the micromachined magnetic devices. However, unlike conventional inductors, the inductance is not proportional to the square of the number of coil turns in the components, since due to fabrication constraints on the micromachined inductive component, larger numbers of coil turns require a longer core length (in a single coil layer design). The important parameter, coupling factor, in micromachined transformers is calculated by

$$K = \frac{L_m}{\sqrt{L_p L_s}}, \qquad L_m = \frac{\mu_0 \mu_r A_c N_p N_s}{\ell_c} \tag{4}$$

where

- L_m mutual inductance;
- L_p primary inductance;
- L_s the secondary inductance.

$$\Phi = B A_c = \frac{NI}{\Re} \Rightarrow I_{\text{sat}} = \frac{B_{\text{sat}} \Re A_c}{N}. \tag{5}$$

Equation (5) shows that the dc saturation current is proportional to the saturation flux density. Permalloy (80% nickel–20% iron) and orthonol (50% nickel–50% iron) are used as core materials to demonstrate the geometry of micromachined magnetic devices. Eddy current losses in the magnetic core as well as the skin depth effect in the conductor are neglected in these calculations.

TABLE I
COMPOSITON OF NICKEL–IRON AND COPPER ELECTROPLATING SOLUTIONS

Nickel-iron electroplating solutions

Component	Fe (20%)	Fe (50%)
$NiSO_4$-$6H_2O$	200 (g/l)	168 (g/l)
$FeSO_4$-$7H_2O$	8 (g/l)	81 (g/l)
$NiCl_2$-$6H_2O$	5 (g/l)	135 (g/l)
H_3BO_3	25 (g/l)	50 (g/l)
Saccharin	3 (g/l)	3 (g/l)
PH	2.5 ~ 3.0	3.5 ~ 4.0
Temperature	25 ~ 30 (°C)	55 ~ 60 (°C)

Copper electroplating solution

Component	Quantity	
$CuSO_4$-$5H_2O$	250 (g/l)	
H_2SO_4	25 (ml/l)	

III. FABRICATION

A. Fabricated Magnetic Core Samples

Micromachined inductors have been realized previously using a *permalloy* (80% nickel–20% iron) core [9]. It is known that other alloy compositions of the nickel–iron system have higher saturation flux densities. For example, the 50% nickel–50% iron alloy, known as *orthonol*, has a saturation flux density on the order of 50% higher than permalloy in the bulk [12]. In order to assess the suitability of orthonol as a magnetic material for micromachined magnetic devices, samples of both permalloy and orthonol were deposited using electroplating and characterized using a vibrating sample magnetometer.

The fabrication procedure for the preparation of core samples is as follows. A seed layer consisting of 200 Å chromium, 1500 Å copper, and 400 Å chromium was deposited on a silicon wafer using electron beam evaporation. A 15 μm thick photoresist layer (Shipley STR-1110) was deposited on top of the seed layer and patterned to form sample molds 12 mm × 4 mm in area. The magnetic materials were then deposited using electroplating using the parameters in Table I. In some cases, electroplating bath additives were used to reduce stress as described below. The core samples were then removed from the wafer using wet chemical etching. In order to assess this effect in actual application, inductive components based on both permalloy and orthonol were fabricated and tested.

IV. INTEGRATED MAGNETIC DEVICES

Among several obstacles encountered in fabricating micromachined inductors and transformers that are to be operated at relatively high currents, the major difficulty comes from the fabrication of thick wrapping coils that have a low conductor resistance. Thick molds for the wrapping coils are patterned using thick photoresist and photolithography. Electroplating is a favorable technique for deposition of thick metal conductors, but electroplating usually requires a plating seed layer that must be removed after completing the fabrication structure. Consequently, the seed layer used for lower conductor lines should serve as the plating seed layer for the via and remain until the fabrication is completed. At this time, the seed layer must be removed or all of the coils will be shorted. Unfortunately, the seed layer is now difficult to remove, as it is at the bottom of the structure. Simple blanket etching to expose the seed layer will not work as the magnetic core placed on the top of the lower conductor lines as a mask to prevent complete exposure of the seed layer. To solve this problem, a mesh-type seed layer [9], [11] is used which can serve as the electroplating seed layer for the lower conductor lines and vias until the fabrication is completed. When the fabrication of these devices is completed, the edges of the mesh-type seed layer can be exposed using plasma etch and then removed, ensuring the electrical isolation of the coils.

Another difficulty in the fabrication comes from the need to fabricate a thick magnetic core (for low magnetic reluctance) which should be placed on the top of the insulated lower conductor lines. The relatively high aspect ratio of the magnetic core causes a serious difficulty in patterning the vias and the upper conductor lines, due to poor planarization of the surface. Another seed layer that has the same shape as the magnetic core is used to solve these problems.

Fig. 2 shows a brief fabrication process of these devices. The process started with a glass substrate. chromium/copper/chromium layers were deposited to form a seed layer for electroplating using electron-beam evaporation. This mesh-type seed layer was patterned to form a conductor network to be removed after serving as the seed layer for plating of the conductor and vias. Polyimide (Dupont PI2611) was spun on the top of mesh-type seed layer to construct electroplating molds for the bottom conductor lines. Four coats were made to obtain 40 μm thick polyimide molds. After coating, the polyimide was cured at 300°C for 1 h in nitrogen. An aluminum layer (0.2 μm thick) was deposited on top of the cured polyimide as a hard mask for dry etching. Molds for lower conductor lines were patterned and plasma etched until the seed layer was exposed. After etching the aluminum hard mask and the top chromium of the seed layer, the molds were filled with electroplated copper using standard electroplating techniques and the copper electroplating solution shown in Table I.

One coat of polyimide was cast to isolate the lower conductor lines and the magnetic core. The seed layer was deposited, mesh-patterned, coated with polyimide (35 μm thick), and hard-cured. An aluminum layer (0.2 μm thick) was deposited as a hard mask for dry etching. A mold for the magnetic core was patterned and etched until the seed layer was exposed. After etching the aluminum hard mask and the top chromium of the seed layer, the mold was filled with plated nickel–iron using standard electroplating techniques. The nickel–iron alloy plating solutions and conditions are shown in Table I. To plate the orthonol core [Ni (50%)–Fe (50 %) alloy], various additives from M&T Chemicals, Inc., were optionally used to control internal stress and ductility of the deposit, to keep the iron content solublized, and to obtain bright film and leveling of the process. The pH and temperature should be kept within the recommended

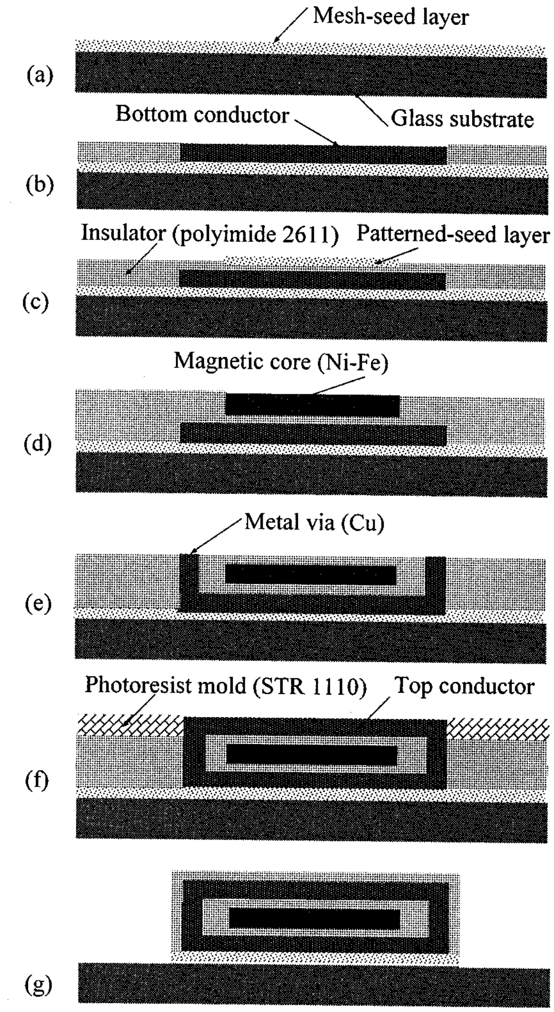

Fig. 2. Fabrication procedure for micromachined inductors and transformers: (a) patterning of mesh seed layer, (b) electroplating of lower conductors, (c) passivation and patterning of mesh seed layer, (d) formation of mold and electroplating of a magnetic core, (e) via conductor plating, (f) upper conductor plating, and (g) removal of polyimide and mesh seedlay.

limits. A higher value may cause highly stressed deposits and a lower value may reduce leveling and cause chemical dissolving of iron anodes resulting in disruption of the bath equilibrium. Higher than recommended temperatures may give hazy deposits; much lower temperature may cause high current density burning. Air agitation and saccharin were also added to reduce internal stress and to keep the iron content stabilized.

One coat of polyimide was spin-cast and cured to insulate the core and upper conductor lines. Via holes were patterned in a sputtered aluminum mask layer and etched through the polyimide layer using 100% oxygen plasma. Vias were filled with electroplated copper. A copper/chromium seed layer was deposited, and molds for the upper conductor lines were formed using thick photoresist. The molds were filled with plated copper and removed. After removing the seed layer, a polyimide passivation layer was coated and cured to protect the top conductor lines. The polyimide was optionally masked and etched to the bottom. The bottom mesh seed layer was then wet etched. At the completion of fabrication, samples were diced and tested.

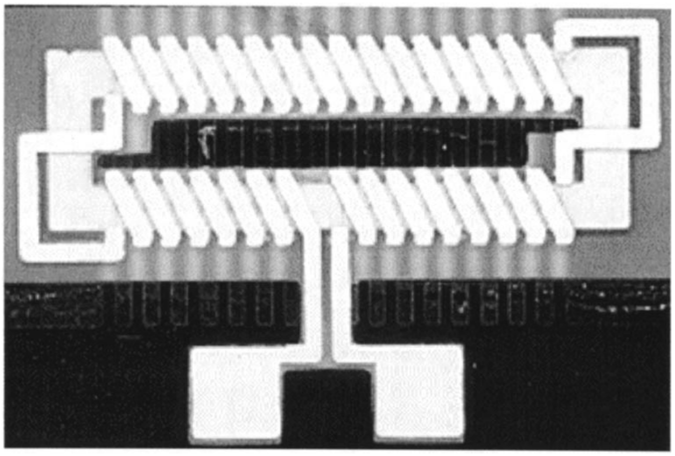

Fig. 3. Photomicrograph of fabricated micromachined inductor. The inductor is 4 mm in length, 1 mm in width, and 0.13 mm in height.

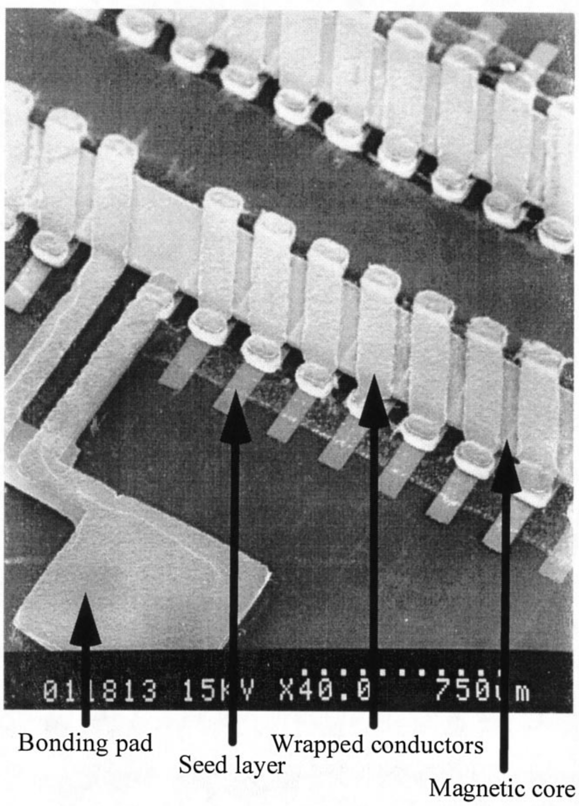

Fig. 4. Scanning electron micrograph of the top view of micromachined inductor.

Fig. 3 shows a micromachined inductor which consists of electroplated copper conductor lines (40 μm thick), an electroplated magnetic core (15 μm thick), and polyimide PI-2611 as an insulation material. Figs. 4 and 5 show wrapped conductors and magnetic core through scanning electron micrographs taken after removing the polyimide. Figs. 6 and 7 show multi-turned micromachined inductors and transformers which consist of electroplated copper conductor lines (40 μm thick), electroplated magnetic core (35 μm), and polyimide PI-2611 as an insulation material. Figs. 8 and 9 show scanning electron micrograph top views of multiturned micromachined inductors and transformers taken after removing the polyimide.

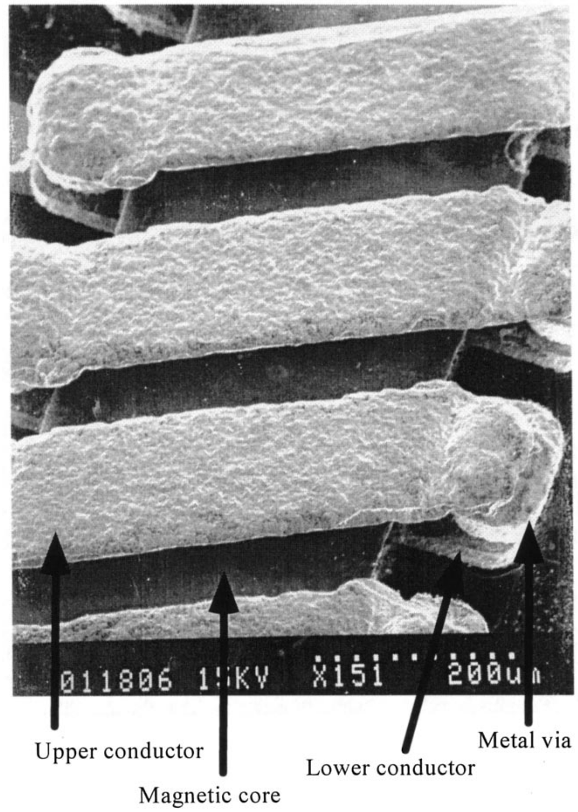

Fig. 5. Scanning electron micrograph of wrapped conductors and core of the micromachined inductor.

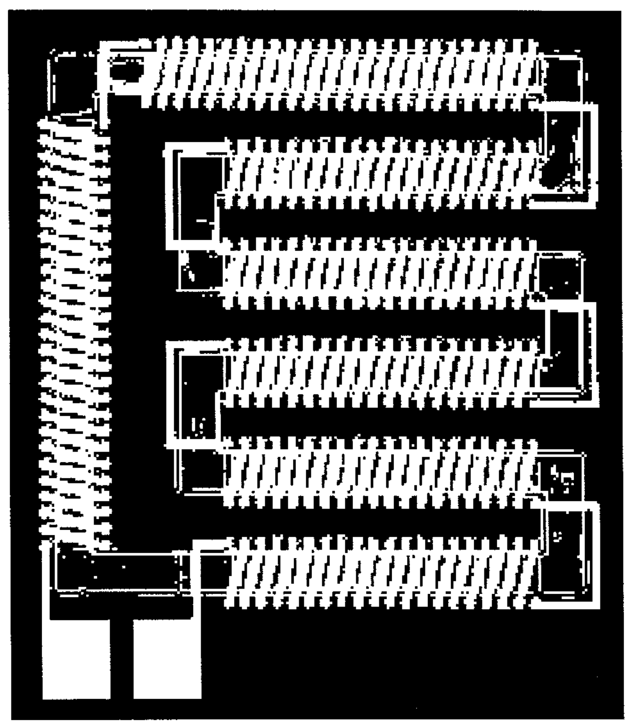

Fig. 6. Photomicrograph of multitumed micromachined inductor with air gap. The inductor is 4 mm in length, 4 mm in width, and 0.13 mm in height.

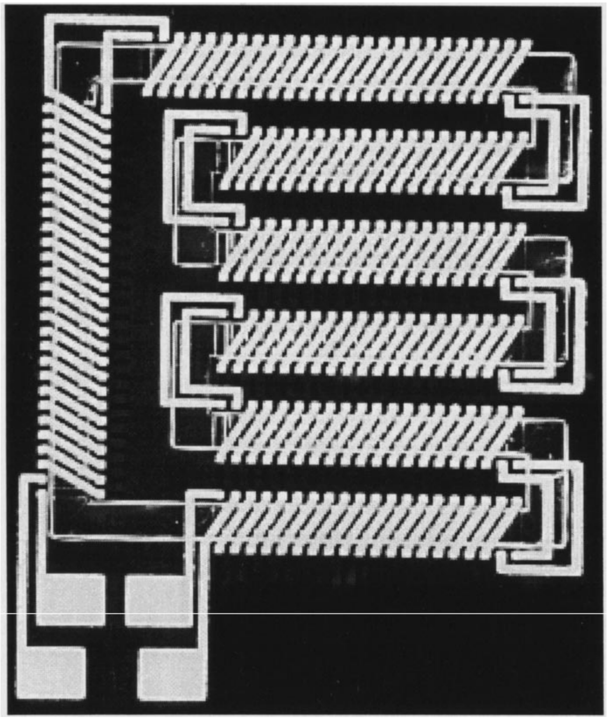

Fig. 7. Photomicrograph of multiturned micromachined transformer with no air gap. The inductor is 4 mm in length, 4 mm in width, and 0.13 mm in height.

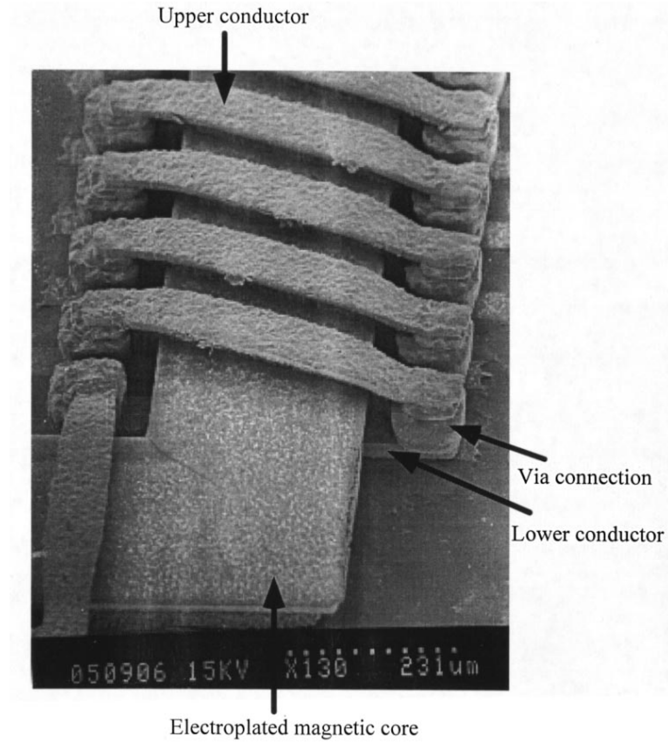

Fig. 9. Scanning electron micrograph of wrapped conductors, vias, and a core of multiturned micromachined inductor.

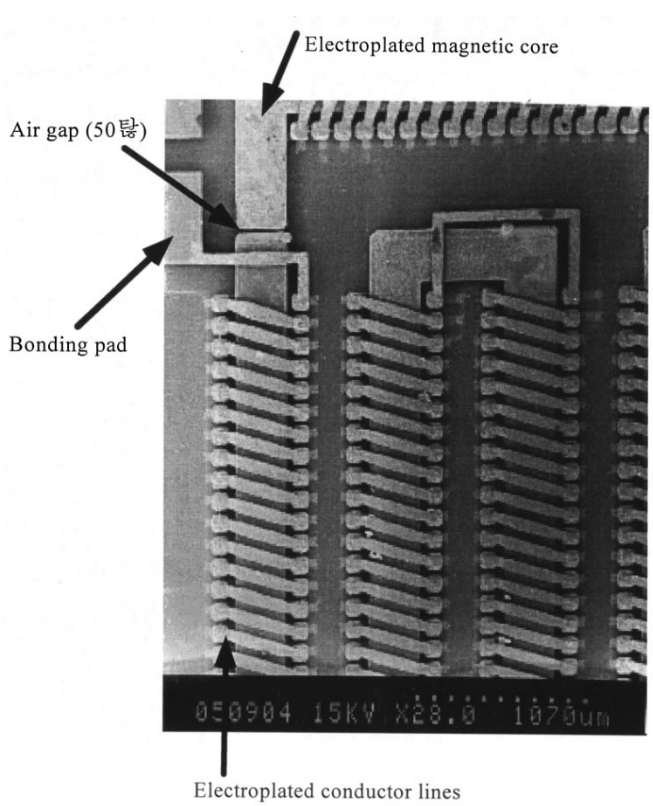

Fig. 8. Scanning electron micrograph of the top view of multiturned micromachined inductor.

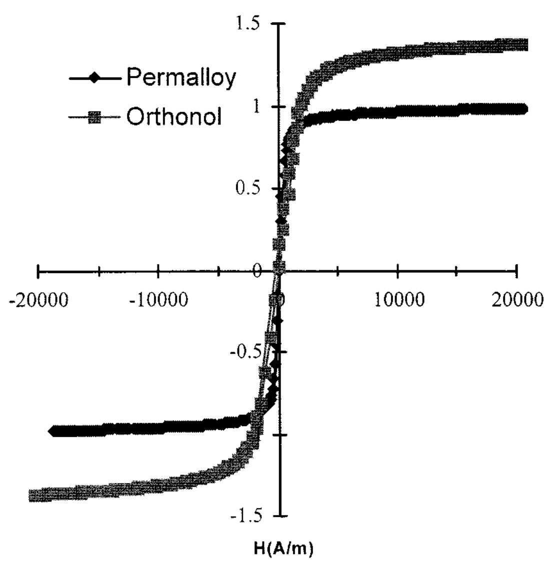

Fig. 10. Flux density versus magnetic field intensity curve for fabricated *permalloy* and *orthonol* test samples.

V. Experimental Results and Analysis

A. Comparison of Magnetic Properties of Core Materials—Permalloy and Orthonol

Fig. 10 shows the magnetic B-H (flux density—magnetic field strength) properties of the permalloy and orthonol materials. Both materials exhibit a relatively high permeability. The saturation flux density for these electroplated permalloy samples is approximately 0.9 T, whereas the saturation flux density for these orthonol samples is approximately 1.35 T.

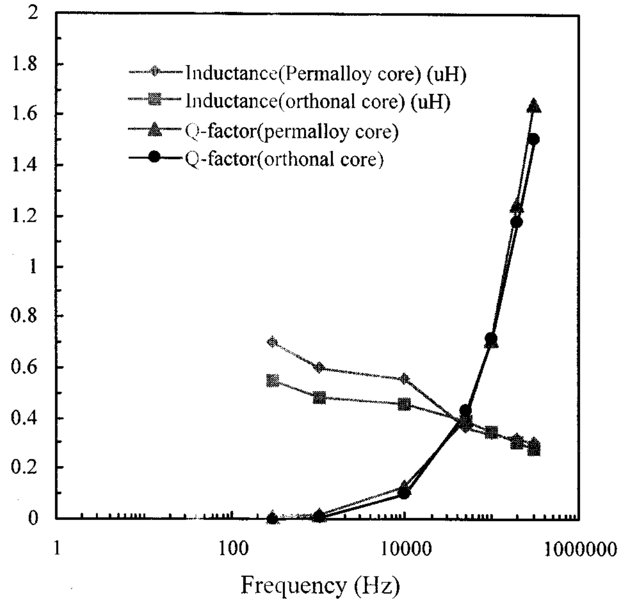

Fig. 11. Comparison of the inductance and the Q-factor of inductors with different magneticcore materials.

From (5), this 40% increase in saturation flux density for orthonol-based magnetic components should translate directly to a 40% increase in saturation current.

B. Comparison of Permalloy and Orthonol Core Inductors

For an inductor size of 4 mm × 1.0 mm × 0.13 mm thickness having 30 turns of multilevel coils, the achieved inductances were approximately 0.67 μH for the inductor with permalloy core and 0.57 μH for the inductor with orthonol core at low frequencies (<1 MHz). Inductance as a function of both frequency and dc current were measured using a Wayne–Kerr 3245 precision inductance analyzer. Fig. 11 shows the inductance and Q-factor of each device as a function of frequency. As seen, the permalloy core inductor has a slightly higher inductance and Q-factor than the orthonol core inductor. The measured dc resistance of both inductors was approximately 0.3 Ω. This is very consistent with the value (0.309 Ω) evaluated from its geometry (neglecting via resistance) and the bulk value of copper conductivity. Although the individual via contact resistance was not measured, the excellent agreement between measured and calculated total resistance indicates that the via resistance is negligibly small. Thus, the electroplated via as predicted has avoided the high via resistance problem.

To find the circuit parameters of the integrated inductors, an equivalent circuit is assumed in which a stray capacitance [16] is in parallel with the series connection of the inductance and the internal resistance. The resistance and stray capacitance of the inductors are derived from the measured impedance and phase as a function of frequency using equivalent circuit analysis and data collected from a Hewlett Packard impedance/gain-phase analyzer 4194A. Fig. 12(a) and (b) show the gain and the phase shift of the micromachined inductors with permalloy and orthonol cores, respectively. Over the frequency range of a few hundred Hz to 10 MHz, the micromachined inductors display behavior similar to that of conventional inductors, with

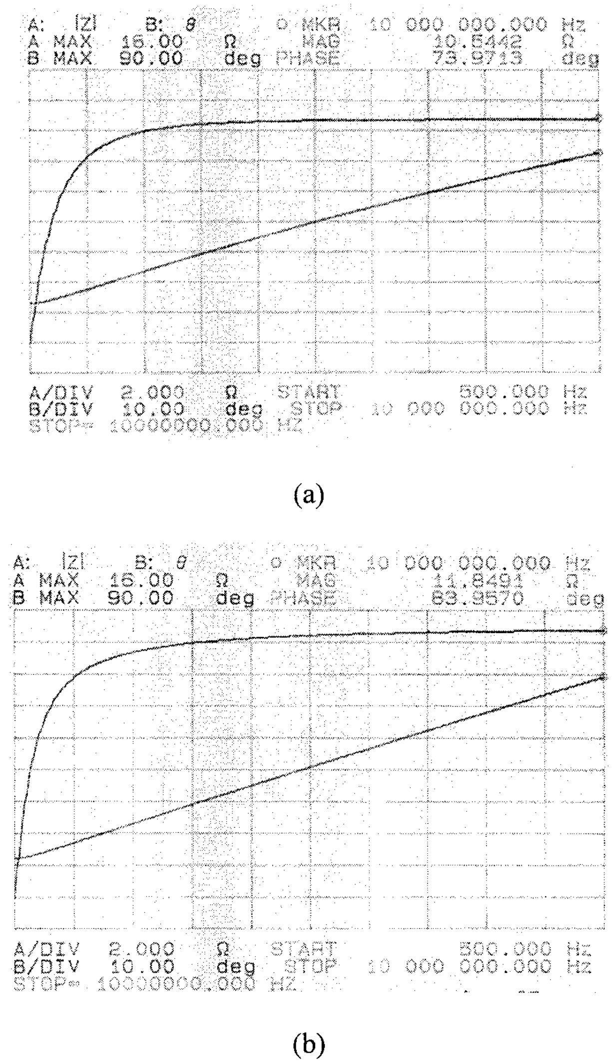

Fig. 12. Impedance and phase analysis of micromachined inductor with (a) permalloy core and (b) orthonol core.

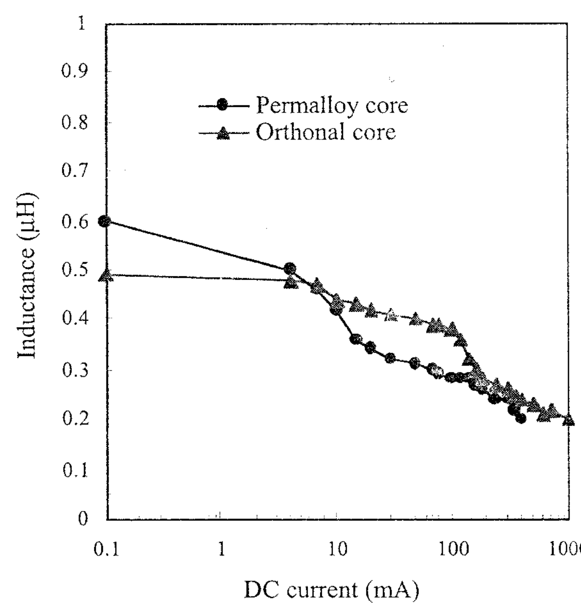

Fig. 13. Comparison of dc saturation current of micromachined inductors with different magnetic core materials.

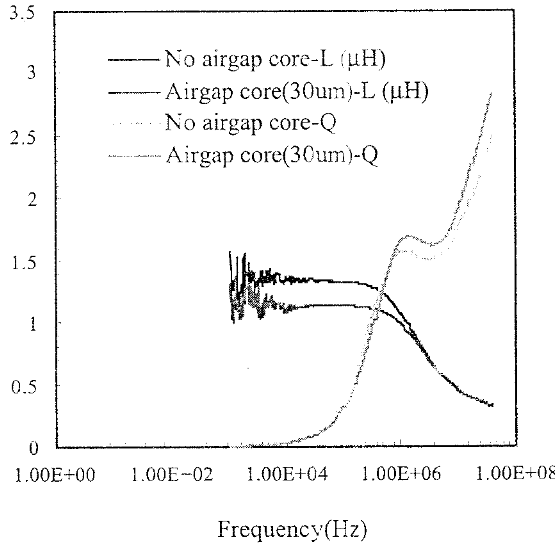

Fig. 14. Comparison of the inductance and the Q-factor of multiturned micromachined inductors.

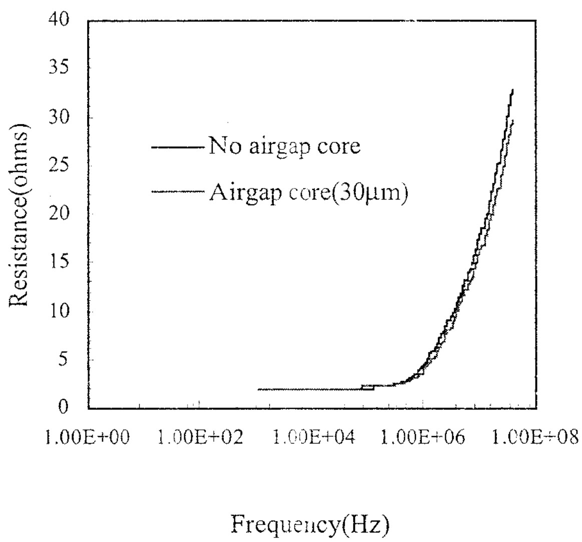

Fig. 15. Comparison of the resistance of multiturned micromachined inductors.

impedance increasing linearly with frequency and phase shifts near 90°. From these data, it can be concluded that winding capacitance and other parasitic capacitance do not appear to significantly affect inductor performance over the frequency ranges measured.

Fig. 13 shows the inductance of each inductor as a function of dc current. dc saturation current (generally defined as the current at which the inductance value falls off 20–30% of the measured inductance without the applied dc current) was measured using a Wayne–Kerr 3245 precision inductance analyzer. The dc saturation current of the orthonol core inductor is much higher than the permalloy core inductor. From these data it can be concluded that orthonol core inductors may perform significantly better than permalloy core inductors in applications requiring magnetic energy storage, such as dc/dc converters.

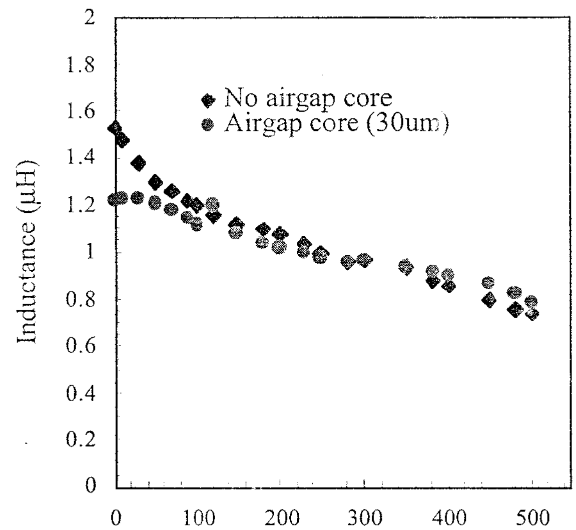

Fig. 16. Comparison of the saturation current of multiturned micromachined inductors.

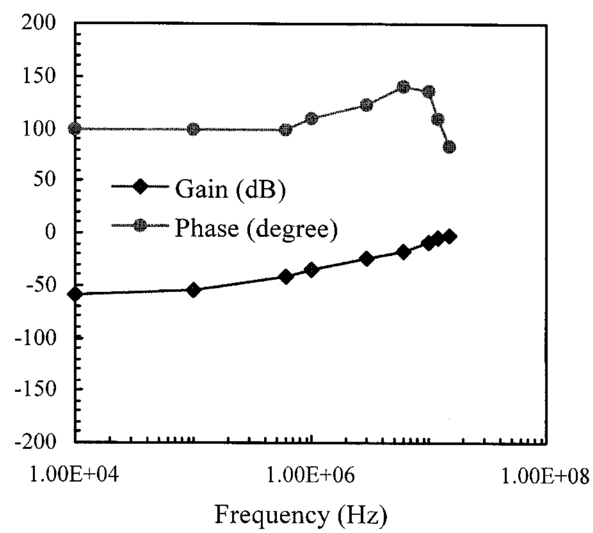

Fig. 17. Gain and phase analysis of multitumed micromachined transformer.

C. Comparison of Multiturned Permalloy Core Inductors with and without Airgap

Once the characteristics of the test sample were determined, characteristics of actual fabricated components were measured. Inductance, resistance, Q-factor, and gain of fabricated inductive components were measured by a Hewlett Packard impedance/gain-phase analyzer 4194A. Fig. 14 shows that at low frequencies, the microinductor ($L = 1.5$ μH) with no airgap has slightly higher inductance than the inductor ($L = 1.3$ μH) with airgap as expected, since the core with no airgap has a lower reluctance than the core with airgap. The inductor with airgap has a higher Q-factor than the no airgap device at higher frequencies as shown in Fig. 14. At higher frequencies, the resistance of the inductor with airgap is lower than that of the one with no airgap as shown in Fig. 15.

DC saturation current, I80 is defined as the current at which the inductance value falls off 20% from the measured inductance without any applied dc current. Fig. 16 shows that the inductor with air gap has much higher saturation current (I80 = 250 mA) than the no airgap device (I80 = 85 mA). Finally, a fully integrated transformer with primary to secondary winding ratio of 1 : 1 has 2 dB loss when operating at 15 MHz as shown in Fig. 17.

VI. CONCLUSION

Fully integrated micromachined inductors and transformers with different magnetic cores and geometries have been fabricated on glass using micromachining techniques. Orthonol and permalloy core inductors have been compared to find a appropriate micromachined inductor for power applications. As predicted, geometrically similar orthonol core inductors have much higher dc saturation current than permalloy core inductors, which is a very important characteristic for power inductors. By comparing microinductors with airgap in the core to devices without airgap in the core, it has been shown that airgap core devices exhibit improved characteristics. Only low temperature processes have been used in fabrication, and the fabrication sequences are packaging-compatible. These micromachined inductors and transfomers have potential application as integrated passives for multichip modules, integrated miniaturized dc/dc power converters and filters, and micromagnetic sensors and actuators integrated with the package.

ACKNOWLEDGMENT

The authors would like to thank the staff at Microelectronics Research Center, Georgia Institute of Technology (Georgia Tech), Atlanta, for carrying out the microfabrication, W. Taylor, Georgia Tech, as well as M. Schneider and H. Baltes, Swiss Federal Institute of Technology (ETH-Zürich), for their assistance with measurement of magnetic properties of materials, and C. H. Ahn, University of Cincinnati and the MEMS Group, Georgia Tech, for valuable technical discussions.

REFERENCES

[1] R. Soohoo, "Magnetic thin film inductor for integrated circuit application," *IEEE Trans. Magn.*, vol. MAG-15, pp. 1803–1805, Nov. 1979.
[2] K. Mizuguchi and K. Yamasawa, "An on-board-type micro-switching converter with MHz band-operation," *IEEE Trans. Magn.*, vol. 9, no. 2, pp. 174–178, 1994.
[3] T. Sato, M. Tomita, A. Sawabe, T. Inoue, T. Mizoguchi, and M. Sahashi, "A magnetic thin film inductor and its application to a MHz switching dc-dc converter," *IEEE Trans. Magn.*, vol. 30, pp. 217–223, Mar. 1994.
[4] T Sato, M. Hasegawa, T. Mizoguchi, and M. Sahashi, "Study of high power planar inductor," *IEEE Trans. Magn.*, vol. 27, pp. 5277–5279, Nov. 1991.
[5] K. Yamasawa, K. Maruyama, I. Hirohama, and P. Biringer, "High frequency operation of a planar-type microtransformer and its application to multilayered switching regulators," *IEEE Trans. Magn.*, vol. 26, pp. 1204–1209, May 1990.
[6] J. Park and M. Allen, "A comparison of micromachined inductors with different magnetic core materials," in *Proc. IEEE 46th Electron. Comp. Technol. Conf.*, Orlando, FL, 1996, pp. 375–381.
[7] O. Oshiro, H. Tsujimoto, and K. Shirae, "A novel miniature planar inductor," *IEEE Trans. Magn.*, vol. MAG-23, pp. 3759–3761, Sept. 1987.
[8] K. Yamaguchi, S. Ohnuma, H. Matsuki, and K. Murakami, "Characteristics of a thin film microtransformer with circular spiral coils," *IEEE Trans. Magn.*, vol. 29, no. 5, pp. 2232–2237, Sept. 1993.
[9] C. Ahn, Y. Kim, and M. Allen, "A Comparison of two micromachined inductors (bar and meander type) for fully integrated boost dc/dc power converters," *IEEE Trans. Power Electron.*, vol. 11, pp. 239–245, Apr. 1996.
[10] H. Nishimura, I. Kamei, K. Shirakawa, Y. Kobayashi, O. Nakajima, and K. Murakami, "Studies on frequency characteristics of micro inductors," *IEEE Trans. Magn.*, vol. 9, pp. 76–82, May 1994.
[11] J. Park and M. Allen, "High current integrated microinductors and microtransformers using low temperature fabrication processes," in *Proc. Int. Symp. Hybrid Microelectron.*, Minneapolis, MN, 1996, pp. 120–125.
[12] M. Greenhouse, "Design of planar rectangular microelectronic inductors," *IEEE Trans. Parts, Hybrids, Packag.*, vol. PHP-10, pp. 101–109, Apr. 1987.
[13] *Transformer and Inductor Design Handbook*, 2nd ed., 1988, pp. 20–25.
[14] C. Ahn and M. Allen, "A fully integrated surface micromachined magnetic microactuator with a multilevel meander magnetic core," *IEEE J. Microelectromech. Syst.*, vol. 2, no. 1, pp. 15–22, Mar. 1993.
[15] K. Kawabe, H. Koyama, and K. Shirae, "Planar inductor," *IEEE Trans. Magn.*, vol. MAG-20, pp. 1804–1806, Sept. 1984.
[16] M Yamaguchi, M. Matsumoto, H. Ohzeki, and K. I. Arai, "Analysis of the inductance and the stray capacitance of the dry-etched micro inductors," *IEEE Trans. Magn.*, vol. 27, pp. 5274–5276, Nov. 1991.

Jae Yeong Park (M'99) received the B.S. degree in telecommunication and information engineering from Hankuk Aviation University, Seoul, Korea, in 1992, and the M.S.E.E. and Ph.D. degrees in electrical and computer engineering from the Georgia Institute of Technology, Atlanta, in 1995 and 1997, respectively.

After 1997, he worked at the Georgia Institute of Technology as a Research Engineer. Currently, he is working at LG Corporate Institute of Technology, Seoul. His interests include the development, design, fabrication, and characterization of microsensorsand microactuators; microstructures and technologies microelectromechanical systems (MEMS) compatible with IC fabrication; developing magnetic materials and deposition methods for micromagnetic devices such as electroplating and screen-printing; planar magnetic microinductors and microtransformers for wireless communications, RF MEMS components and modules, integrated power supplies (power converters and control circuits), and multichip modules; micromachined relays and switches; and micromachined motors.

Dr. Park is a member of IMAPS.

Mark G. Allen received the B.A. degree in chemistry, the B.S.E. degree in chemical engineering, and the B.S.E. degree in electrical engineering from the University of Pennsylvania, Philadelphia, in 1984, and the S.M. and Ph.D. degrees in microelectronic materials from the Massachusetts Institute of Technology (MIT), Cambridge, in 1986 and 1989, respectively.

His research at MIT focused on micromachining techniques to create structures for the *in situ* measurement of mechanical properties and adhesion of thin films for use in microelectronic processing. He was also engaged in microsensors, microactuators, and in feedback-stabilized micromachined mirrors for laser applications. He joined the faculty of the Georgia Institute of Technology, Atlanta, after a postdoctoral appointment at MIT. His current research interests are in the field of micromachining and in microsensorand microactuator fabrication that is compatible with the IC fabrication. Other interests are in micromachined pressure and in acceleration sensors, micromotors, integrated flow valves, piezoelectric materials combined with semiconductor circuits and optical materials, multichip packaging for integrated circuits and microstructures, integration of organic piezoelectric materials with semiconductor circuits for sensing and actuation and materials, and mechanical property issues in micromachining.